Disassembly of Amyloid Fibrils by Premicellar and Micellar Aggregates of a Tetrameric Cationic Surfactant in Aqueous Solution

ARTICLE *in* LANGMUIR · MARCH 2011

Impact Factor: 4.46 · DOI: 10.1021/la200350j · Source: PubMed

Langmuir

ARTICLE

pubs.acs.org/Langmuir

Disassembly of Amyloid Fibrils by Premicellar and Micellar Aggregates of a Tetrameric Cationic Surfactant in Aqueous Solution

Chengqian He, Yanbo Hou, Yuchun Han, and Yilin Wang*

Key Laboratory of Colloid and Interface Science, Beijing National Laboratory for Molecular Sciences, Institute of Chemistry, Chinese Academy of Sciences, Beijing 100190, People's Republic of China

ABSTRACT: We report a finding that not only the micelles but also the premicellar aggregates of a star-like tetrameric quaternary ammonium surfactant PATC can disassemble and clear mature β-amyloid Aβ(1−40) fibrils in aqueous solution. Different from other surfactants, PATC self-assembles into network-like aggregates below its critical micelle concentration (CMC). The strong self-assembly ability of PATC even below its CMC enables PATC to disaggregate the Aβ(1−40) fibrils far below the charge neutralization point of the Aβ(1−40) with PATC. There may be two key features of the fibril disassembly induced by the surfactant. First, the positively charged surfactant molecules bind with the negatively charged Aβ(1−40) fibrils through electrostatic interaction. Second, the self-assembly of the surfactant molecules bound onto the Aβ(1−40) fibrils disaggregate the fibrils, and the surfactant molecules form mixed aggregates with the Aβ(1−40) molecules. The result reveals a structural approach of constructing efficient disassembly agents to mature β-amyloid fibrils.

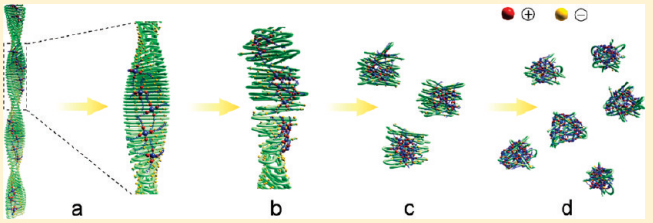

INTRODUCTION

Alzheimer's disease (AD) is a significant health issue in contemporary society, and its impact will continue to increase as the population ages. However, current drugs for AD do not prevent or reverse the disease and provide only modest symptomatic benefits. Driven by the clear unmet medical need and the growing knowledge of the molecular pathophysiology of Alzheimer's disease, the number of agents in development has increased dramatically in recent years. In 1991, Hardy et al.[1] proposed that β-amyloid (Aβ) deposits were the fundamental cause of AD. Mechanisms aimed at preventing or reversing accumulation of amyloid deposits are being actively pursued,[2] and knowledge of the details of Aβ metabolism and plaque formation,[3] hyperphosphorylation of tau, and the formation of tangles[4] is constantly expanding. Lines of research of disease-modifying drug therapies including Aβ clearance from the brain and the inhibition of Aβ production and aggregation into plaques are underway.[5] According to the amyloid hypothesis, it is accepted that protein misfolding and subsequent amyloid fibril formation are directly linked to the pathogenesis of a group of human disorders known as amyloidoses.[6] It seems that one of the potential goals in the prevention or therapy of Alzheimer's disease is to decrease or eliminate neuritic plaques composed of fibrillar β-amyloid.[7] An intriguing finding[8] published in 1999 described that Aβ42 immunization of affected PDAPP transgenic mice could remarkably reduce AD-related neuropathologies. It was also demonstrated that the immunization treatment resulted in the clearance of preexisting Aβ amyloid deposits, which might account for the recovery of pathology. Besides antibodies,[9−11] numerous small molecules have recently been reported as disaggregation agents of Aβ fibril, including rifampicin[12] and dopamine,[13] which contain aromatic groups. Yet the subsequent clinical trials showed the cytotoxicity of these compounds was of great concern.[14−16] So the exploration of various effective and safe approaches for fibril disassembly is still necessary and exigent.

Previously, we found cationic gemini surfactant hexamethylene-1,6-bis (dodecyl dimethylammonium bromide) ($C_{12}C_6C_{12}Br_2$) can regulate the fibrillogenesis.[17] $C_{12}C_6C_{12}Br_2$ micelles decrease the Aβ(1−40) nucleation rate and inhibit the lateral association between fibrils. Contrarily, both the Aβ(1−40) nucleation rate and the lateral association between fibrils are greatly promoted by the $C_{12}C_6C_{12}Br_2$ monomers. It was also found that $C_{12}C_6C_{12}Br_2$ micelles can effectively disassemble mature Aβ(1−40) fibrils in vitro.[18] Aβ fibrils are disaggregated into soluble substances and simultaneously transported small molecules to prevent further formation of Aβ fibrils. There might be two key factors for the surfactants inducing Aβ fibril disassembly, which are positive charges and strong self-aggregation ability. On the basis of these two points, we hope to design a new kind of cationic surfactant with lower critical micelle concentration (CMC) to reduce the surfactant amount required for Aβ fibril disaggregation. Finally, we got a tetrameric quaternary ammonium surfactant, N^1,N^{16}-didodecyl-7,10-bis(3-(2-(dodecyldimethylammonio)ethylamino)-3-oxopropyl)-N^1,N^1,N^{16},N^{16}-tetramethyl-4,13-dioxo-3,7,10,14-tetraazahexadecane-1,16-diaminium tetrabromide (PATC),[19] whose CMC is 0.08 mM. Moreover, it was found to show very special aggregation behavior. PATC has four hydrophobic chains and charged

Received: January 26, 2011
Revised: March 8, 2011
Published: March 25, 2011

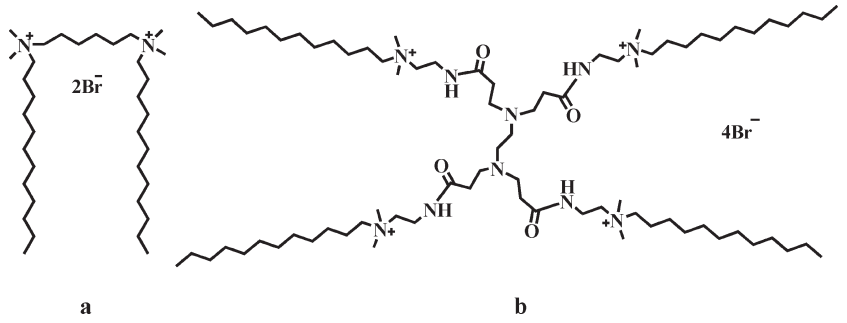

Figure 1. Molecular structures of (a) $C_{12}C_6C_{12}Br_2$ and (b) PATC.

hydrophilic headgroups connected by amide-type spacer group. Because of its high charge density, strong electrostatic repulsion causes the headgroups to leave each others as far as possible, accompanyied by the hydrocarbon chains stretching out. This generates a star-shaped molecular configuration of PATC below its CMC. Especially based on this configuration, PATC molecules form large premicellar network-like aggregates far below the CMC through hydrophobic interaction among the hydrophobic chains of the different molecules. Hence, we are curious whether PATC with such a special self-assembly ability can disaggregate the fibrils and block the Aβ fibrillization even at the concentration below its CMC. It will verify and consummate our mode for the fibril disassembly.[18]

In the present work, the effect of the tetrameric quaternary ammonium surfactant PATC on the disaggregation behavior of Aβ(1−40) fibrils has been investigated by thioflavin T (ThT) fluorescence, Fourier transform-infrared spectroscopic (FT-IR) technique, and atom force microscopy (AFM) under a physiological pH condition of 7.4. $C_{12}C_6C_{12}Br_2$ was selected to be the reference compound at the same concentrations as PATC. Obviously, the selected two surfactants have different molecular structures as shown in Figure 1. ThT fluorescence was used to study the variation of the Aβ(1−40) fibril contents upon the addition of $C_{12}C_6C_{12}Br_2$ monomers, $C_{12}C_6C_{12}Br_2$ micelles, PATC premicellar aggregates, and PATC micelles. Fourier transform-infrared (FT-IR) spectroscopic technique was utilized to monitor the secondary structure of the fibrils with the surfactants of different concentrations. AFM was used to investigate the morphology change of the Aβ(1−40) fibrils in the disaggregation process. This study shows that PATC is a powerful medium for disassembling the Aβ(1−40) fibrils even at 0.02 mM, which is far below its CMC. The comparison with the $C_{12}C_6C_{12}Br_2$ monomers suggests that the disassembly effectiveness of PATC premicellar aggregates might be attributed to the strong self-aggregation ability of PATC below its CMC. Although cationic compounds are not a right choice in treating AD because they cannot pass through blood brain barrier, the present result reveals a structural approach of constructing efficient disassembly agents to mature β-amyloid fibrils.

EXPERIMENTAL SECTION

Materials. Amyloid β(1−40) (trifluoroacetate salt) (Aβ(1−40), code, 4307-v; lot, 590708) was purchased from Peptide Institute Inc. (Japan). The purity of the peptide was greater than 95%. Gemini surfactant hexamethylene-1,6-bis(dodecyldimethylammonium bromide) ($C_{12}C_6C_{12}Br_2$) was synthesized and purified according to the method of Zana et al.[20] N^1,N^{16}-Didodecyl-7,10-bis(3-(2-(dodecyldimethylammonio)ethylamino)-3-oxopropyl)-N^1,N^1,N^{16},N^{16}-tetramethyl-4,13-dioxo-3,7,10,14-tetraazahexadecane-1,16-diaminium tetrabromide (PATC) was synthesized as described previously.[19] The structures of $C_{12}C_6C_{12}Br_2$ and PATC were characterized by ^{1}H NMR spectroscopy, mass spectroscopy, and the purity was verified by elemental analysis and surface tension measurements. 1,1,1,3,3,3-Hexafluoro-2-propanol (HFIP) was from ACROS. All of the experiments were carried out in phosphate buffer of pH 7.4 with ionic strength (I) of 10 mM. Pure water was obtained from the Milli-Q equipment.

Amyloid β(1−40) Preparation. Aβ(1−40) in nonaggregated form was prepared as described previously.[17] Briefly, a stock solution was prepared by dissolving ∼0.52 mg of Aβ(1−40) in 600 μL of HFIP, which was incubated at room temperature for 1 h in sealed vials. Next, the solution was bath-sonicated for 30 min until Aβ(1−40) dissolved completely. After that, HFIP was removed from the disaggregated peptide by evaporation under a gentle stream of nitrogen. Just before the following experiments were initiated, an aliquot of Aβ(1−40) was dissolved in 3.0 mL of phosphate buffer with ion concentration of 10 mM (pH 7.4). The molecular weight of Aβ(1−40) is about 4.3 kD. The final peptide molar concentration is ∼40 μM. The solutions were then kept at 30 °C for the following experiments.

Formation and Disaggregation of Mature Aβ(1−40) Fibrils. Aβ(1−40) fibrils were prepared in a sealed vial by stirring (90 rpm) for 1 week at 30 °C. For the fibril disaggregation experiment, the prepared fibrils were mixed with phosphate buffer, the $C_{12}C_6C_{12}Br_2$, and PATC solutions of different concentrations, respectively. The Aβ(1−40) concentration remains at 39 μM. The mixtures were then shaken for several minutes and incubated at 30 °C. The samples were withdrawn at the different time intervals for measurements.

ThT Fluorescence. Fluorescence measurements were carried out with a Hitachi F-4500 spectrophotometer. A drop (10 μL) of sample was withdrawn and added to 1 mL of 10 μM ThT buffer solution. Immediately the fluorescence intensity was measured at an excitation wavelength of 440 nm, and emission spectra were scanned from 460 to 560 nm. The fluorescence intensity of solvent blank was subtracted. The widths of both the excitation slit and the emission slit were set to 5 nm. A quartz cell with 1 cm path length was used. The intensity was normalized to blank control experiment.

Atomic Force Microscopy (AFM). A Multimode Nanoscope IIIa AFM (Digital Instruments, CA) was used for AFM imaging. For ambient imaging, 3−5 μL of Aβ(1−40) sample solution was deposited onto a freshly cleaved piece of mica and left to adhere for 5−10 min. The sample was then briefly rinsed with Milli-Q water and dried with a gentle stream of nitrogen. Probes used were etched silicon probes attached to 125 μm cantilevers with nominal spring constant of 40 N/m (Digital Instruments, model RTESPW). All provided morphology images were recorded using a tapping mode at 512 × 512 pixel resolution and a scan speed of 1.0−1.8 Hz. Topographic data were regularly recorded in both trace and retrace to check on scan artifacts. They were shown in the height mode without any image processing except flattening. Analysis of

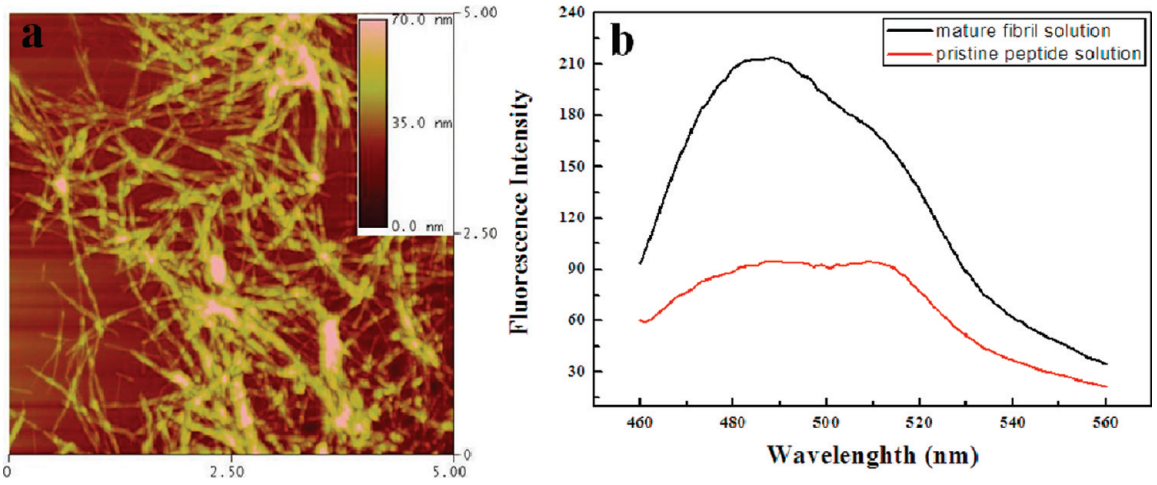

Figure 2. The characteristics of the prepared Aβ(1−40) fibrils. (a) AFM images (5 × 5 μm^2) of the mature Aβ(1−40) fibrils. (b) ThT fluorescence emission spectra (λ_{excit} = 440 nm) of pristine peptide solution and mature Aβ(1−40) fibril solution.

the images was carried out using the Digital Instruments Nanoscope Software (Version 512r2). All of the samples were prepared and observed at least five times.

Fourier Transform-Infrared Spectroscopic (FT-IR). Samples were prepared by evaporating a 10 μL drop of sample on CaF_2 glass slides, then were dried in vacuum, followed by buffer exchanging with D_2O and dehydration (repeated twice). Spectra were measured with a Bruker Optics TENSOR-27 FT-IR spectrophotometer. The extracted amide I band contour was subjected to the second derivative calculation and Gaussian curve-fitting analysis. After decomposition of the amide I band (1700−1600 cm^{-1}), the secondary structure contents were estimated using the criteria described by Pelton and Mclean.[21]

RESULTS AND DISCUSSION

Mature Aβ(1−40) fibrils were prepared following well-established protocols and were confirmed from the characterization of ThT fluorescence and AFM (Figure 2). The AFM images reveal the presence of abundant fibrils with diameter of 5−10 nm and length ranging from tens nanometers to a few micrometers (Figure 2a). The resultant fibril samples produced a marked intensity gain of ThT fluorescence at ∼486 nm wavelength as compared to the pristine peptide solution prior to the fibril formation (Figure 2b), indicating the presence of ordered fibril structures. Although some reports have evidenced that the ThT dye is not only specific to the amyloid fibrils but also specific to some other protein fibrils, the variation of the relative intensity of ThT fluorescence can still reflect the change of the amount of the Aβ(1−40) fibrils in the present system studied.[22]

The disassembly efficiencies of the mature Aβ(1−40) fibrils by using PATC and $C_{12}C_6C_{12}Br_2$ at the concentrations below and above their CMC were compared. After being mixed with the fibril solutions, the surfactant concentrations were separately 0.02 and 1.16 mM for both $C_{12}C_6C_{12}Br_2$ and PATC. The concentrations are below and above the CMC respectively, because the CMC values are 1.0 mM for $C_{12}C_6C_{12}Br_2$ and 0.08 mM for PATC. The Aβ(1−40) fibril concentration remains at 39 μM. So the selected surfactant concentrations made the comparison available among the disassembly efficiencies of the Aβ(1−40) fibrils induced by micelles, premicellar aggregates, and surfactant monomers. Figure 3 presents the variations of the corresponding ThT fluorescence intensity at 486 nm as a function of time (λ_{excit} = 440 nm). Both $C_{12}C_6C_{12}Br_2$ and PATC micelles caused prominent reduction of ThT fluorescence intensity, about 70% and 60% decrease within 1 h. Moreover, the relative intensity almost reached to zero after 95 h. However, $C_{12}C_6C_{12}Br_2$ monomers at 0.02 mM only caused a slight decease in ThT fluorescence intensity, and the fluorescence intensity started to increase with time after about 95 h. The fluorescence intensity of the Aβ(1−40) fibrils mixed with phosphate buffer without any surfactants also deceased in the first 95 h and then increased with time. It suggests that the dilution of the Aβ(1−40) fibril solution induced a slight disaggregation, but the fibrillogenesis was not blocked. As compared to the phosphate buffer, $C_{12}C_6C_{12}Br_2$ monomers act as a promoter of the fibril formation, which is similar to the results we reported before.[17] Especially, the PATC premicellar aggregates at 0.02 mM caused a rapid, significant, and continuous reduction of ThT fluorescence intensity as the $C_{12}C_6C_{12}Br_2$ and PATC micelles did at 1.16 mM. Because all of the surfactant aggregates and monomers themselves have no effect on the ThT fluorescence intensity (data not shown), the change of ThT fluorescence intensity quantitatively reflects the change of the fibril content.[23] Therefore, the sharp decreases of ThT fluorescence caused by the cationic surfactants,

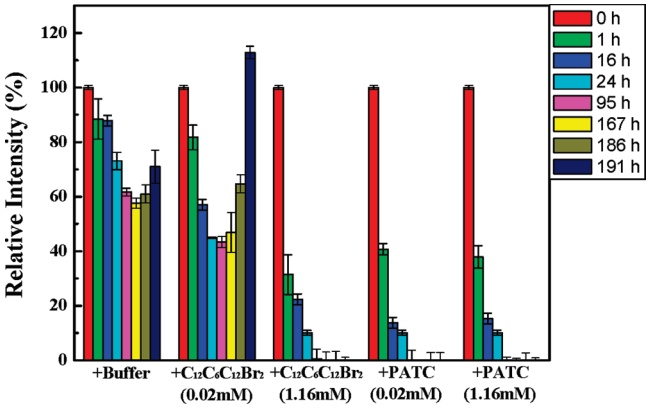

Figure 3. ThT fluorescence results showing the dependence of the Aβ(1−40) fibril content on time in the presence of 0.02 mM $C_{12}C_6C_{12}Br_2$, 1.16 mM $C_{12}C_6C_{12}Br_2$, 0.02 mM PATC, and 1.16 mM PATC.

dx.doi.org/10.1021/la200350j |*Langmuir* 2011, 27, 4551–4556

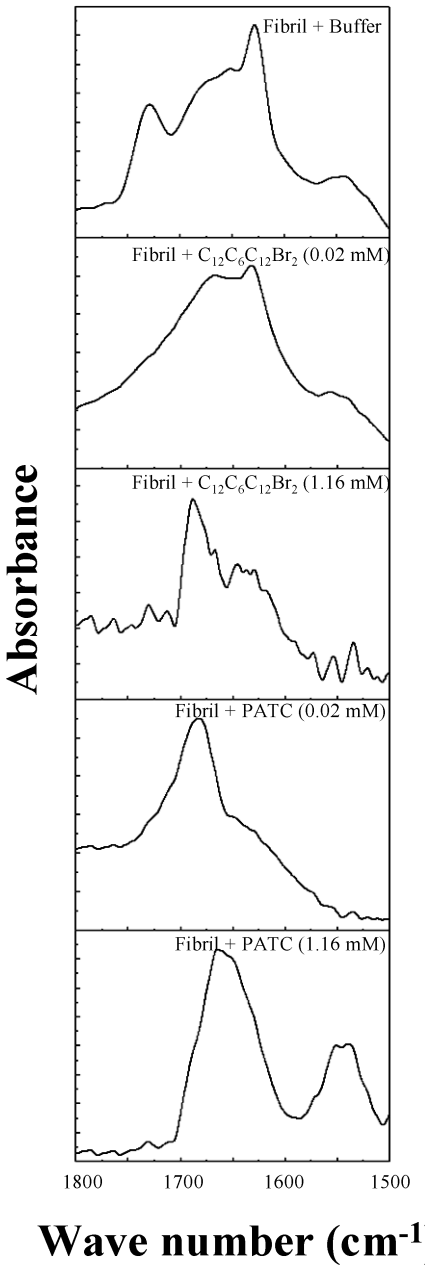

Figure 4. FT-IR spectra of the mixtures of Aβ(1−40) fibrils with buffer, 0.02 mM $C_{12}C_6C_{12}Br_2$, 1.16 mM $C_{12}C_6C_{12}Br_2$, 0.02 mM PATC, or 1.16 mM PATC in the 1800−1500 cm^{-1} region.

that is, $C_{12}C_6C_{12}Br_2$ and PATC micelles and PATC premicellar aggregates, indicate the significant disassembly process of the Aβ(1−40) fibrils. The ThT fluorescence results show PATC has very strong disassembling ability no matter whether below or above the CMC. The disaggregation ability of PATC to the Aβ(1−40) fibrils at 0.02 mM might be related to its ability of forming network-like aggregates below its CMC.[19]

To study the structural transitions of the Aβ(1−40) fibrils induced by mixing with the surfactant solutions, the FT-IR spectroscopic technique was used to explore the changes of the secondary structure of the Aβ(1−40) fibrils (Figure 4). After decomposition of the amide I band (1700−1600 cm^{-1}), the secondary structure contents were estimated (Table 1). The Aβ(1−40) fibril solution mixed with buffer showed the β-sheet structure is the major component, which is a structural characteristic of the amyloid fibrils. Yet the addition of $C_{12}C_6C_{12}Br_2$ or PATC into the fibril solution changed the secondary structure of the fibrils. The β-sheet and α-helix contents decreased accompanied by the increase of the turn content when the Aβ(1−40) fibril solutions were mixed with 1.16 mM $C_{12}C_6C_{12}Br_2$, 1.16 mM PATC, or 0.02 mM PATC separately. On the contrary, the β-sheet content remained nearly unchanged with the addition of 0.02 mM $C_{12}C_6C_{12}Br_2$. These results indicate the Aβ(1−40) conformation were transferred by $C_{12}C_6C_{12}Br_2$ micelles, PATC micelles, and PATC premicellar aggregates, from ordered β-sheet to loose-turn conformation. This result also confirmed the disaggregation of Aβ(1−40) fibrils by the PATC even below its CMC, which agrees well with the ThT fluorescence result.

We compared the overall morphology transitions of the Aβ(1−40) fibrils in the $C_{12}C_6C_{12}Br_2$ solutions with those in the PATC solutions by AFM (Figure 5). The $C_{12}C_6C_{12}Br_2$ and PATC micelles and the PATC premicellar aggregates partly broke the Aβ(1−40) fibrils in the first hour (Figure 5B1,D1, C1). Only a small amount of thin or short fibrils was caught in the scanned images. Many breakage points appeared along the Aβ(1−40) fibrils, and they gradually spread. After 24 h, all of the original long fibrils disappeared, leaving only small aggregates of varying sizes (Figure 5B2,D2,C2). However, the situation was totally different when the $C_{12}C_6C_{12}Br_2$ concentration was below its CMC. Figure 5 A1 shows that the mixture of the Aβ(1−40) fibril solution with the $C_{12}C_6C_{12}Br_2$ monomers presents the mature fibrils all along. In the eighth day (more than 191 h), the amount of the mature Aβ(1−40) fibrils even became significantly more than that in the first day. All of the AFM results are well consistent with the above ThT and FT-IR measurements, strongly proving that the PATC can disassemble the mature Aβ(1−40) fibrils and transform the fibrils into irregular aggregates even with the concentration below its CMC.

Although more detailed kinetic studies are needed to fully understand the mechanism of the fibril disassembly, the observations above still provide some understanding. At pH 7.4, Aβ(1−40) peptide carries negative charges,[24] while both PATC and $C_{12}C_6C_{12}Br_2$ are cationic. If the positive charges of the surfactants are in excess of the Aβ(1−40) negative charges, electrostatic repulsion among the peptide fibrils might be strengthened. Also, the fibril association will be inhibited. However, the number of positive charges of 0.02 mM PATC is about 1/3 of the number of the negative charges of the Aβ(1−40). The cationic surfactant molecules bind on the Aβ(1−40) molecules through electrostatic interaction, but the positive charges are not enough to strengthen the electrostatic repulsion between the fibrils. Therefore, we consider that the strong self-aggregation ability of PATC is one of the key factors of disassembling the Aβ(1−40) fibrils. The AFM images showed the fibrils disassembled into small particles step-by-step. It may be reasonable to envision the following disassembly scenario for the PATC premicellar aggregates (Figure 6). Upon mixing, the PATC monomers will be bound on the fibril surface arising primarily from electrostatic interaction. At the same time, PATC with the star-shaped configuration should be favor to form the network-like aggregates as we reported before.[19] It could be described as a struggle between the PATC aggregates and Aβ fibrils. The result is that the Aβ(1−40) molecules were reorganized and associated with the PATC molecules, ultimately leading to the formation of nanoscopic mixed aggregates. To sum, we believe that the special

dx.doi.org/10.1021/la200350j |*Langmuir* 2011, 27, 4551–4556

Table 1. Secondary Structure Contents of the Aβ(1-40) Fibrils Mixed with $C_{12}C_6C_{12}Br_2$ and PATC at Different Concentrations Using the FT-IR Technique

	α-helix (%)	β-sheet (%)	random (%)	β-turn (%)
fibril + buffer	19	61	6	14
fibril + $C_{12}C_6C_{12}Br_2$ (0.02 mM)	20	59	3	18
fibril + $C_{12}C_6C_{12}Br_2$ (1.16 mM)	11	33	10	46
fibril + PATC (0.02 mM)	3	34	13	50
fibril + PATC (1.16 mM)	13	34	9	44

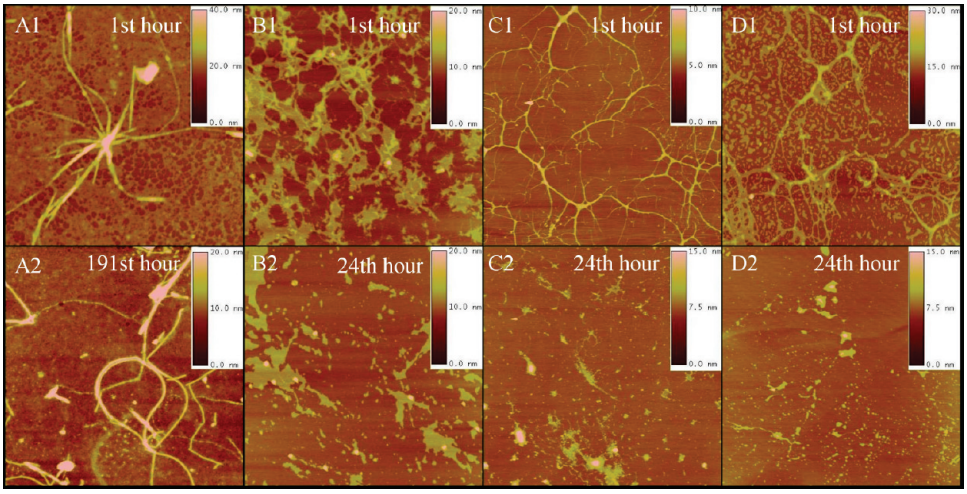

Figure 5. The effects of the $C_{12}C_6C_{12}Br_2$ and PATC with different concentrations on the morphologies of the Aβ(1−40). AFM images ($5 \times 5\,\mu m^2$) for the mixtures of Aβ(1−40) fibrils with $C_{12}C_6C_{12}Br_2$ and PATC at the different time intervals. (A) $C_{12}C_6C_{12}Br_2$ (0.02 mM); (B) $C_{12}C_6C_{12}Br_2$ (1.16 mM); (C) PATC (0.02 mM); and (D) PATC (1.16 mM).

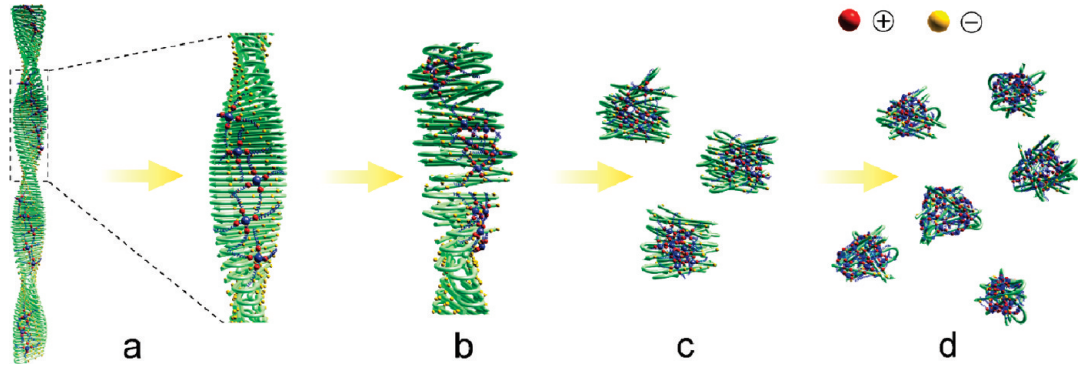

Figure 6. The proposed mechanism of the PATC premicellar aggregates disassembling the Aβ(1−40) fibrils. (a) PATC molecules bind on the fibril surface through electrostatic interaction. (b,c) Fibril breaks into pieces due to the premicellar network-like aggregation of PATC. (d) Complete disassembly of the fibrils and formation of mixed aggregates.

molecular structure of PATC and its resultant strong self-assembly ability is the main reason that the PATC premicellar aggregates are a strong disassembly medium for the Aβ(1−40) fibrils.

CONCLUSIONS

The present work studies the effect of tetrameric quaternary ammonium surfactant PATC and cationic gemini surfactant $C_{12}C_6C_{12}Br_2$ on the disassembly of the Aβ(1−40) fibrils above and below their CMC. The results show that both PATC micelles and premicellar aggregates can effectively disassemble mature Aβ(1−40) fibrils in aqueous solution, which is sustained and thorough. This ability is still strong at the PATC concentration as low as 0.02 mM, while $C_{12}C_6C_{12}Br_2$ loses disassembly efficacy at the concentration. The significant self-aggregation ability of PATC below the CMC should be the key factor in the fibril disassembly. This result would have critical implications for understanding the process of the fibril disaggregation. Although the cationic surfactants cannot pass through the blood brain barrier, the finding is still helpful to reveal the approaches of the

dx.doi.org/10.1021/la200350j |*Langmuir* 2011, 27, 4551–4556

Aβ(1−40) fibril disassembly. To further optimize the surfactant biocompatibility and delivery efficiency, we are pursuing new surfactant systems with different binding modalities on the Aβ(1−40) peptide.

AUTHOR INFORMATION

Corresponding Author
*E-mail: yilinwang@iccas.ac.cn.

ACKNOWLEDGMENT

This work is supported by National Natural Science Foundation of China (21025313, 20973181, 50821062, and 21021003).

REFERENCES

(1) Hardy, J.; Allsop, D. *Trends Pharmacol. Sci.* **1991**, *12*, 383–388.
(2) Jhee, S.; Shiovitz, T.; Crawford, A. W.; Cutler, N. R. *Expert Opin. Invest. Drugs* **2001**, *10*, 593–605.
(3) Yan, P.; Bero, A. W.; Cirrito, J. R.; Xiao, Q. L.; Hu, X. Y.; Wang, Y.; Gonzales, E.; Holtzman, D. M.; Lee, J. M. *J. Neurosci.* **2009**, *29*, 10706–10714.
(4) Brandt, R.; Gergou, A.; Wacker, I.; Fath, T.; Hutter, H. *Neurobiol. Aging* **2009**, *30*, 22–33.
(5) Blennow, K.; de Leon, M. J.; Zetterberg, H. *Lancet* **2006**, *368*, 387–403.
(6) Porat, Y.; Abramowitz, A.; Gazit, E. *Chem. Biol. Drug Des.* **2006**, *67*, 27–37.
(7) Gordon, D. J.; Sciarretta, K. L.; Meredith, S. C. *Biochemistry* **2001**, *40*, 8237–8245.
(8) Schenk, D.; Barbour, R.; Dunn, W.; Gordon, G.; Grajeda, H.; Guido, T.; Hu, K.; Huang, J. P.; Johnson-Wood, K.; Khan, K.; Kholodenko, D.; Lee, M.; Liao, Z. M.; Lieberburg, I.; Motter, R.; Mutter, L.; Soriano, F.; Shopp, G.; Vasquez, N.; Vandevert, C.; Walker, S.; Wogulis, M.; Yednock, T.; Games, D.; Seubert, P. *Nature* **1999**, *400*, 173–177.
(9) Solomon, B.; Koppel, R.; Frankel, D.; HananAharon, E. *Proc. Natl. Acad. Sci. U.S.A.* **1997**, *94*, 4109–4112.
(10) DeMattos, R. B.; Bales, K. R.; Cummins, D. J.; Dodart, J. C.; Paul, S. M.; Holtzman, D. M. *Proc. Natl. Acad. Sci. U.S.A.* **2001**, *98*, 8850–8855.
(11) Mamikonyan, G.; Necula, M.; Mkrtichyan, M.; Ghochikyan, A.; Petrushina, I.; Movsesyan, N.; Mina, E.; Kiyatkin, A.; Glabe, C. G.; Cribbs, D. H.; Agadjanyan, M. G. *J. Biol. Chem.* **2007**, *282*, 22376–22386.
(12) Li, J.; Zhu, M.; Manning-Bog, A. B.; Di Monte, D. A.; Fink, A. L. *FASEB J.* **2004**, *18*, 962–964.
(13) Li, J.; Zhu, M.; Rajamani, S.; Uversky, V. N.; Fink, A. L. *Chem. Biol.* **2004**, *11*, 1513–1521.
(14) Winters, W. D.; Tuan, A. L.; Morton, D. L. *Cancer Res.* **1974**, *34*, 3173–3179.
(15) Wersinger, C.; Sidhu, A. *Neurosci. Lett.* **2003**, *342*, 124–128.
(16) Fent, K.; Hunn, J. *Mar. Environ. Res.* **1996**, *42*, 377–382.
(17) Cao, M. W.; Han, Y. C.; Wang, J. B.; Wang, Y. L. *J. Phys. Chem. B* **2007**, *111*, 13436–13443.
(18) Han, Y. C.; He, C. Q.; Cao, M. W.; Huang, X.; Wang, Y. L.; Li, Z. B. *Langmuir* **2010**, *26*, 1583–1587.
(19) Hou, Y.; Han, Y.; Deng, M.; Xiang, J.; Wang, Y. L. *Langmuir* **2010**, *26*, 28–33.
(20) Zana, R.; Benrraou, M.; Rueff, R. *Langmuir* **1991**, *7*, 1072–1075.
(21) Pelton, J. T.; McLean, L. R. *Anal. Biochem.* **2000**, *277*, 167–176.
(22) Levine, H. *Protein Sci.* **1993**, *2*, 404–410.
(23) Nilsson, M. R. *Methods* **2004**, *34*, 151–160.
(24) Ma, K.; Clancy, E. L.; Zhang, Y. B.; Ray, D. G.; Wollenberg, K.; Zagorski, M. G. *J. Am. Chem. Soc.* **1999**, *121*, 8698–8706.